JOC The Journal of Organic Chemistry

Article

pubs.acs.org/joc

Synthesis and Optical and Electronic Properties of Core-Modified 21,23-Dithiaporphyrins

Ashley D. Bromby, Ryan P. Jansonius, and Todd C. Sutherland*

Department of Chemistry, University of Calgary, 2500 University Drive NW, Calgary, Alberta, Canada

Supporting Information

ABSTRACT: Core-modified 21,23-dithiaporphyrins, *meso*-substituted with both electron-withdrawing 4-phenylcarboxylic acids and related butyl esters, and electron-donating phenyldodecyl ethers were synthesized. The porphyrins displayed broad absorbance profiles that spanned from 400 to 800 nm with molar absorptivities ranging from 2500 to 200000 M^{-1} cm^{-1}. Electrochemical experiments showed the dithiaporphyrins undergo two consecutive, one-electron, quasi-reversible oxidations and reductions at −1.78, −1.43, 0.63, and 0.91 V versus a ferrocene/ferrocenium internal standard. Spectroelectrochemistry and cyclic voltammetry revealed the dithiaporphyrins are stable and can endure many cycles of oxidation and reduction without signs of decomposition. The electronics of the two dithiaporphyrins were similar, and DFT calculations showed the HOMO−LUMO energy difference was smaller than tetrapyrrolic porphyrin analogues. Overall, the combination of desirable electronics, namely: quasi-reversible oxidations and reductions as well as broad absorbance profiles, combined with stability, imply that these core-modified 21,23-dithiaporphyirns could be potentially used as an ambipolar material for organic electronic applications.

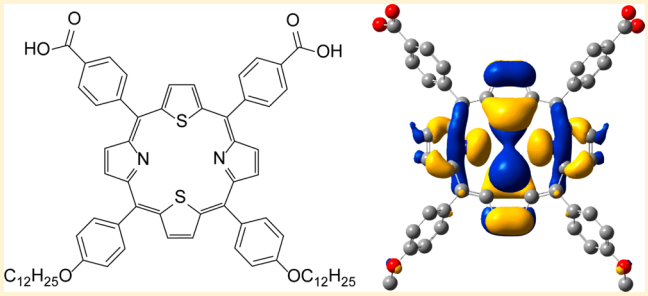

INTRODUCTION

There has been much attention awarded to organic semiconducting materials as flexible, cost-effective, and processable alternatives to inorganic devices for applications including organic light emitting diodes (OLEDs), organic field effect transistors (OFETs), and organic photovoltaic devices (OPVs).[1−4] There are two main approaches to organic electronic materials, namely polymeric and small molecule. Each approach has their own advantages and disadvantages with respect to solution processability, purity, film morphology, and deposition technique. A critical feature common to all of the organic electronic applications is the ability to conduct charges, whether they are holes, electrons, or both, efficiently over large distances (micrometers). Among the families of organic semiconductors, p-type, or hole-conducting materials are more numerous, while their counterpart, n-type, or electron-conducting materials are fewer.[5−10] There is a clear need to synthesize new compounds that can conduct electrons. Furthermore, ambipolar materials, capable of both electron and hole conduction, have the fewest examples in literature to date.[11−14] Ambipolar materials[15] have advantages over unipolar materials in both OFET designs for certain types of logic circuits and OLED applications.[16−20] The typical strategy used to design ambipolar materials is to create blends of both p- and n-type polymers or to covalently link p- and n-type molecules, termed the donor−acceptor approach. Although the blending strategy has shown success, it would be highly advantageous and simpler to create a single molecule capable of both hole and electron transport since microcrystallinity and phase separation are large obstacles to overcome in physical blends. For these reasons, molecular entities that can be both reversibly and readily oxidized and reduced are highly sought as candidates for ambipolar materials.

Porphyrins are highly conjugated, aromatic macrocycles that possess broad absorbance profiles with high molar absorptivities and desirable redox properties and are easily functionalized for electronic tuning. Porphyrin photochemical and electrochemical properties have garnered much interest[16,21−23] regarding a variety of organic device applications. Porphyrins, and particularly core-modified porphyrins, show reversible oxidation and reduction reactions, which is an indicator of ambipolar characteristics, and they have also shown promising charge-transport properties in the solid state.[16,24−31] This contribution reports the synthesis and electronic properties of two core-modified 21,23-dithiaporphyrins which have been nonsymmetrically *meso*-functionalized. The optical properties were assessed by UV−vis absorption and fluorescence experiments, and the ground-state redox properties were assessed by cyclic voltammetry (CV), which were compared to DFT-calculated MO energy levels. Finally, spectroelectrochemistry was carried out to assess the optical properties of both the radical anion and cations.

Received: December 14, 2012
Published: February 5, 2013

 © 2013 American Chemical Society dx.doi.org/10.1021/jo302707f | J. Org. Chem. 2013, 78, 1612−1620

Scheme 1. Synthesis of 21,23-Dithiaporphyrins[a]

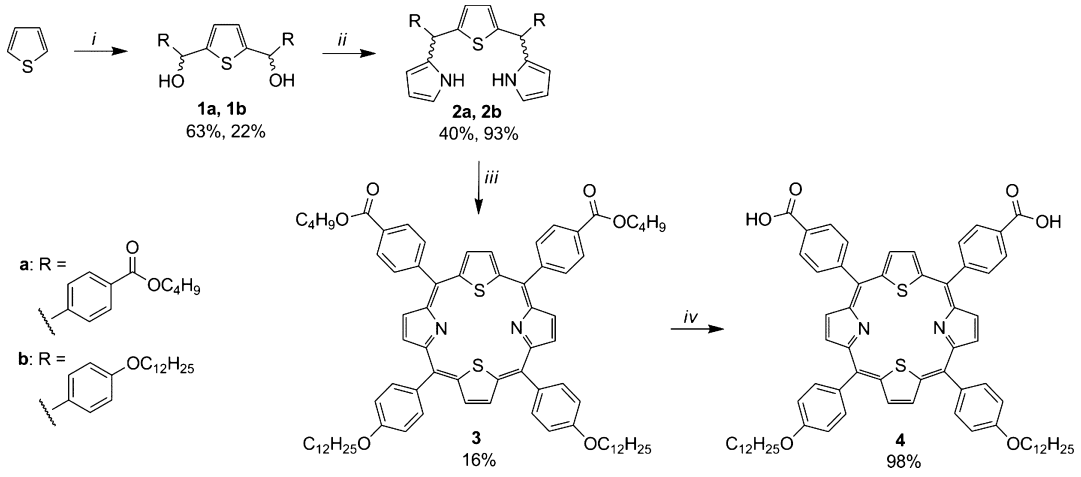

[a]Key: (i) (1) 2.2 equiv of *n*-BuLi and TMEDA; (2) 2.2 equiv of benzaldehyde **a**/**b**; (ii) excess pyrrole and $BF_3{\cdot}OEt_2$ (cat); (iii) (1) thiophenediol **1b** with thiatripyrrane **2a** and $BF_3{\cdot}OEt_2$ (cat.) (note: **2b** does not react with **1a** to form **3** cleanly under these conditions); (2) DDQ (iv) LiOH.

RESULTS AND DISCUSSION

Synthesis. The synthesis began with diol formation, **1a** or **1b**, as shown in Scheme 1 by adding 2 equiv of *n*-BuLi and TMEDA to thiophene to deprotonate the α positions forming the dilithiated intermediate.[32] The dilithiated thiophene was then quenched by the addition of 2 equiv of the desired *meso*-position aldehyde, resulting in diols **1a** and **1b** isolated as a mixture of diastereomers in 63% and 22% yield, respectively. The diastereomeric mixture was not separated as the chiral centers become the final sp^2-hybridized *meso*-positions upon aromatization to the porphyrin. The alkoxyphenyl aldehyde was obtained using standard Williamson ether conditions beginning with 4-hydroxybenzaldehyde following our previous work,[32] and the butyl 4-formylbenzoate was synthesized by reacting 4-formylbenzoic acid in basic conditions with *n*-bromobutane.[33]

It is feasible to synthesize non-symmetric porphyrins by reacting diols **1a** and **1b** with 1 equiv of pyrrole; however, yields suffer and scrambling of the *meso*-positions can occur, leading to challenging separations. To achieve a reasonable porphyrin yield, an additional synthetic step was taken to avoid scrambling of the dithiaporphyrin core. Based on the procedure by Bhat et al.,[34] either thiophene diol **1a** or **1b** was condensed with excess pyrrole in the presence of $BF_3{\cdot}OEt_2$ to form the thiatripyrrane **2a** or **2b** in 40% and 93% yield, respectively, as a diastereomeric mixture. To afford the nonsymmetrically substituted *meso*-positions there are two approaches that could result in dithiaporphyrin **3**, namely reacting **2a** with **1b** or reacting **2b** with **1a**. Interestingly, only the former reaction sequence, **2a** with **1b** in the presence of BF_3 etherate and DDQ,[33,36] resulted in a reasonable yield of **3** (16%).[32,35,36] By starting with **2b**, en route to dithiaporphyrin **3**, the Lewis acid ring-closing step with diol **1a** caused *meso*-position scrambling. The ^{1}H NMR following the reaction of **2b** with diol **1a** after aromatization showed minimal desired porphyrin **3** and appreciable quantities of the symmetric dithiaporphyrin core functionalized with four dodecyloxyphenyl chains. Presumably, the thiophenes functionalized with electron-donating groups are more able to stabilize the carbocation-like intermediates resulting from the loss of pyrrole from the thiatripyrrane. Finally, saponification of dithiaporphyrin **3** using LiOH in a 1:1 (water/THF) solvent mixture afforded dicarboxylate **4** at near-quantitative yields of 98%. Hence, a versatile route to nonsymmetric *meso*-substituted dithiaporphyrins was achieved using electron-deficient thiatripyrranes.

Electronic Absorption and Emission. The absorption spectrum of **4** in DMF is shown in Figure 1 and displays a typical porphyrin profile.[32,35−37] The Soret band for **4** is at 440 nm ($\varepsilon = 2.4 \times 10^5$ M^{-1} cm^{-1}) with less intense Q-bands, shown in Figure 1 inset, at 518 nm, 554 nm, 637 and 701 nm with molar absorptivities of 2.5×10^4 M^{-1} cm^{-1}, 1.4×10^4 M^{-1} cm^{-1}, 1.4×10^3 M^{-1} cm^{-1}, and 6.9×10^3 M^{-1} cm^{-1}, respectively. Expectedly, the absorption spectrum of **3** was nearly identical to **4**, and the optical data are summarized Table 1. Furthermore, both porphyrins **3** and **4** presented Q-bands that were linear in absorbance for concentrations ranging from micro- to millimolar implying minimal aggregation in DMF, and **3** showed linear absorbance behavior in methylene chloride and insignificant solvatochromic effects. Compared to tetrapyrrolic porphyrin analogues,[36] dithiaporphyrins **3** and **4** display red-shifted absorbance maxima, and this observation is consistent with the incorporation of thiophene moieties into the aromatic core.[32] The parent, tetraphenyldithiaporphyrin ($TP\text{-}N_2S_2$), shows similar molar absorptivity trends with peak

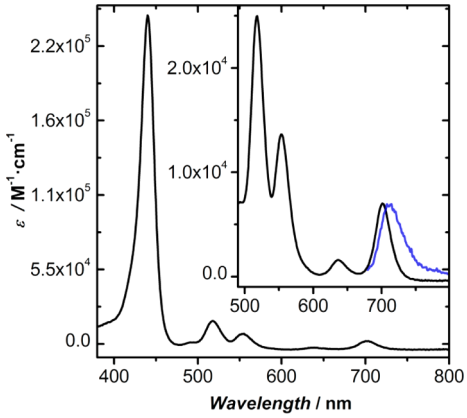

Figure 1. UV−vis absorption spectrum of **4** (1×10^5 M) in DMF (black line). Inset: the expanded Q-band region (black line) and the normalized emission spectrum of **4** (blue line) in DMF.

dx.doi.org/10.1021/jo302707f | J. Org. Chem. 2013, 78, 1612−1620

Table 1. UV-Vis Absorption and Fluorescence Data for 3 and 4[a]

	Soret	Q IV	Q III	Q II	Q I	λ_{max}^{em}	Stokes shift	E_g^{opt} (eV)[d]
3[b]	440 (192)	517 (20)	553 (10)	638 (2.5)	702 (5.1)	714	239	1.75
3[c]	441 (193)	518 (20)	554 (11)	637 (2.3)	701 (5.5)	714	259	1.75
4[c]	440 (242)	518 (25)	554 (14)	637 (1.4)	701 (6.9)	715	279	1.75

[a]Note: Absorption data are shown in nanometers followed by molar absorptivities in parentheses with units of 10^3 L·mol^{-1}·cm^{-1}. Emission data given in nanometers and Stokes shift data in wavenumbers. [b]Spectrum recorded in methylene chloride. [c]Spectrum recorded in N, N-dimethylformamide. [d]Determined by the intersection of the absorption the emission spectra in respective solvent.

maxima at the following wavelengths in chloroform:[37] 435 nm (Soret), 515 nm (Q IV), 548 nm (Q III), 635 nm (Q II), and 699 nm (Q I). The small changes in peak maxima of either **3** or **4** compared to TP-N_2S_2 is attributed to the small electronic contribution that the *meso*-phenyl groups exert on the aromatic macrocyclic N_2S_2 core.

The expanded Q-band region and normalized emission spectrum of dithiaporphyrin **4** is shown in the inset of Figure 1, and the optical data are summarized in Table 1. Excitation at the Soret-band ($S_0 \rightarrow S_2$) or the Q-bands ($S_0 \rightarrow S_1$) II to IV resulted in the same emission profile, indicating efficient relaxation to the lowest energy S_1 state. Both dithiaporphyrins **3** and **4** displayed a small Stokes shift (~260 cm^{-1}) with an emission maximum at 714 nm that was insensitive to solvent changes. Expectedly, the optically determined HOMO−LUMO energy transition was very similar between the related dithiaporphyrins at 1.75 eV (706 nm), as determined by the intersection of the absorption and the emission spectra.

The parent compound, TP-N_2S_2, has similar emission properties, which demonstrates the FMOs are only slightly modified by the noncoplanar *meso*-phenyl substituents.

Electrochemistry. Nonmetalated, free-base, tetrapyrrolic porphyrins exhibit two stepwise, one-electron, reversible oxidations[36,38] and reduction reactions.[39] In methylene chloride, dithiaporphyrin **3** displays four sets of quasi-reversible redox peaks, two one-electron oxidations, and two one-electron reductions as shown in Figure 2. The half-wave reduction and oxidation potentials, summarized in Table 2, are −1.78, −1.43, 0.63, and 0.91 V versus a ferrocene/ferrocenium (Fc/Fc^+) internal standard. Two tetrasubstituted 21,23-dithiaporphyrins bearing symmetric alkoxyphenyl groups were synthesized previously by our group,[32] and the oxidation reactions were studied under similar electrochemical conditions leading to half potentials of 0.47 and 0.67 V versus Fc/Fc^+. Compared to our previous symmetric dithiaporphyrins, porphyrin **3** requires a more anodic potential to oxidize by 0.16 V, presumably attributed to the installation of two electron-withdrawing phenyl ester functional groups that replaced the phenyl ether groups. In addition, the difference between half-wave oxidation potentials of the radical cation and dication in our previous work was 0.20 V compared to 0.28 V for **3**, suggesting a destabilization of the dication caused by the introduction of the two pendant diester functionalities. The reported two, one-electron oxidation half-potentials for metal-free, tetraphenyl porphyrins (H_2TPP) are 0.4 and 0.7 V versus Fc/Fc^+,[39] which is 230 mV less anodic for the first oxidation then **3**, which shows the replacement of two nitrogen heteroatoms with sulfurs within the aromatic core causes a stabilization of the HOMO energy. Dithiaporphyrin **3** was also shown to have two consecutive, one-electron reduction reactions at values similar to the analogous TP-N_2S_2 (−1.44 V and −1.71 V vs versus Fc/Fc^+) measured under similar electrochemical conditions.[40] Metal-free tetraphenylporphyrins (H_2TPP) have a reported

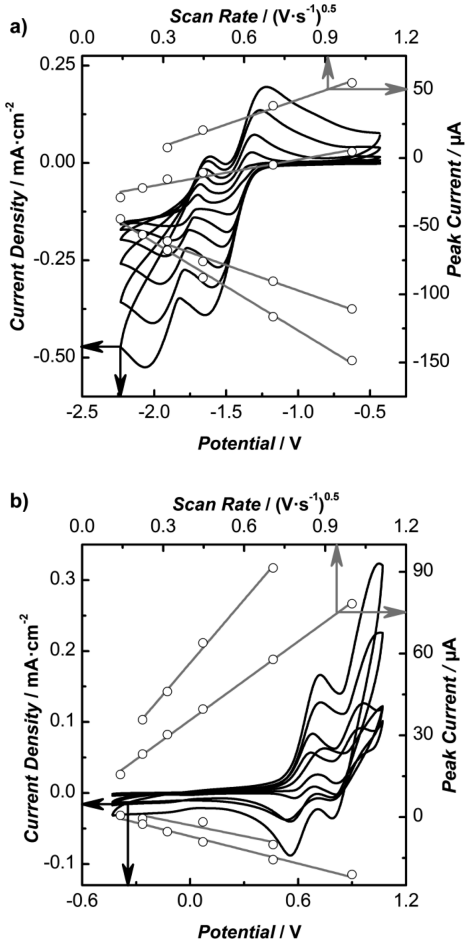

Figure 2. Cyclic voltammograms of (a) reduction region and (b) oxidation region of **3** (2 mM) in methylene chloride containing 0.1 M (nBu)$_4$NPF$_6$ at a glassy carbon electrode at scan rates of 50, 100, 200, 500, and 1000 mVs^{-1} vs Fc/Fc^+. Linear plots show peak current dependence on the square root of the scan rate.

two-electron reduction with half-potentials of −2.17 and −1.86 V versus Fc/Fc^+,[39] which shows dithiaporphyrin **3** is easier to reduce by approximately 0.4 V than its tetrapyrrolic analogue. The incorporation of two sulfur heteroatoms into the aromatic macrocyclic core and the addition of two ester functionalities cause a lowering of the LUMO energy compared to a similarly substituted all-nitrogen porphyrin and highlight these compounds as potential ambipolar materials. The reason the sulfur incorporation causes a lowering of the LUMO energy arises from an trans-annular S···S bonding interaction, which allows the sulfurs to act as an "electron drain"[40] on the macrocyclic aromatic π-system.[41] Single-crystal measurements of TP-N_2S_2 show an intramolecular S···S distance of 3.05 Å[42] as compared to the sum of van der Waals radii at 3.7 Å.

dx.doi.org/10.1021/jo302707f | J. Org. Chem. 2013, 78, 1612−1620

Table 2. Electrochemical Properties for 3 and 4[a]

	$E^{red2}_{1/2}$	$E^{red1}_{1/2}$	$E^{ox1}_{1/2}$	$E^{ox2}_{1/2}$	HOMO[e] (eV)	LUMO[e] (eV)	E_g^{CV}(eV)[f]
3[a]	−1.78	−1.43	0.63	0.91	−5.43	−3.37	1.9
3[b]		−1.33[d]	0.60[c]		−5.40	−3.47	1.9
4[b]		−0.92[d]	0.50[c]		−5.30	−3.88	1.8

[a]Note: Electrochemical experiments were carried out in methylene chloride. [b]Note: Electrochemical experiments were carried out in *N*,*N*-dimethylformamide containing 0.1 M $(n\text{Bu})_4\text{NPF}_6$ with a glassy carbon working electrode, a Ag wire reference electrode, and a Pt wire counter electrode. All potentials are referenced to Fc/Fc^+. Half potentials are given in units of V. [c]Irreversible oxidation, half potential given as estimated onset. [d]Quasi-reversible half potential. [e]Calculated based on the Fc/Fc^+ E_{HOMO} = −4.8 eV.[48,49] [f]Calculated by the difference between HOMO and LUMO.

The peak currents for all of the voltammograms (see the Supporting Information for additional voltammograms of **3** and **4**) show a linear relationship with the square root of the scan rate, which is consistent with a diffusion-controlled reaction, indicating that **3** and **4** do not physisorb to the glassy carbon electrode. Using Nicholson's method,[43] the electron-transfer rate constants for the quasi-reversible reduction and oxidation peaks for **3** were determined to be 1.8×10^{-4} cm s^{-1} (E_{red2}), 4.0×10^{-4} cm s^{-1} (E_{red1}), 4.6×10^{-4} cm s^{-1} (E_{ox1}), and 3.9×10^{-4} cm s^{-1} (E_{ox2}), respectively, and are similar to other dithiaporphyrins and porphyrins.[32,36] Additional electrochemical properties for **3** and **4** are summarized in Table 2 and Table S1 in the Supporting Information.

Interestingly, the two-electron reversible oxidation of **3** in CH_2Cl_2 became irreversible for both dithiaporphyrins **3** and **4** when evaluated in DMF and the reduction of **3** in DMF exhibited peak separations nearing 800 mV, negating electron-transfer rate determinations. Porphyrins are known to undergo chemical reactions once oxidized to the dicationic state, in the presence of nucleophiles, to form isoporphyrins;[44−47] however, the cyclic voltammograms of both **3** and **4** do not support formation of an isoporphyrin but do suggest that a chemical reaction occurs following oxidation in the presence of DMF, leading to an electrochemically silent compound on the reverse scan. At faster scan rates (Figure S6, Supporting Information) there is evidence of a small anodic peak (return to neutral porphyrin) suggesting a slow chemical reaction follows the oxidation to the dication. At slower scan rates, this return wave disappears as the chemical reaction out-competes the return electrochemical oxidation reaction to the neutral porphyrin. No efforts were made to identify the oxidative decomposition products in DMF.

The HOMO−LUMO energy difference for **3** was determined both optically and electrochemically using the onset of absorption and the onsets of the first reduction and oxidation potentials, respectively. Optical and electrochemical methods yielded similar HOMO−LUMO energy gaps of 1.75 and 1.9 eV, respectively, and compare favorably with TP-N_2S_2 at 1.7 eV and H_2TPP at 1.8 eV.[41]

Spectroelectrochemistry. Spectroelectrochemical experiments were carried out to understand the electronic transitions involving both the single-electron, oxidized **3** and the single-electron, reduced **3** in methylene chloride. Figure 3 shows the evolution of the absorption spectra of **3** in a thin-layer optically transparent electrochemical cell[50] during oxidation to the radical cation and during reduction to the radical anion. During the one-electron oxidation to the radical cation (Figure 3a), dithiaporphyrin **3** shows a marked decrease in the Soret band at 440 nm concomitant with a large new band growing in at 468 nm. In addition, Figure 3a shows several isosbestic points, which supports a clean conversion to the radical cation with few

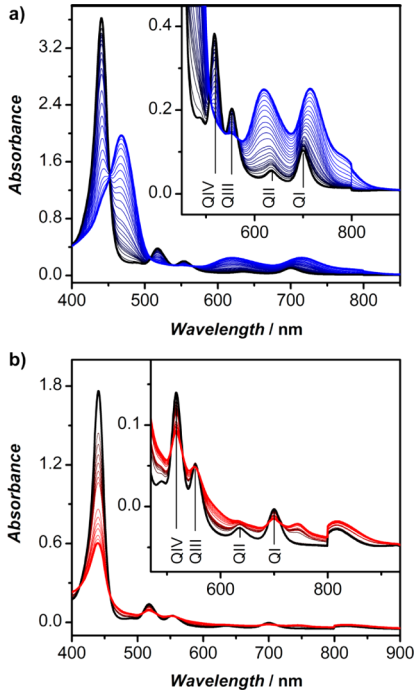

Figure 3. Spectroelectrochemistry spectra of neutral **3** (black line), (a) oxidized cation 3^+ (blue line), and (b) reduced anion 3^- (red line) in methylene chloride containing 0.1 M $(n\text{Bu})_4\text{NPF}_6$.

side products. In the Q-band region, **3** shows the disappearance of Q III and Q IV bands upon oxidation and the growth of three spectral features at 621 nm, 715 nm and a shoulder at 778 nm. Importantly, the spectrum for neutral porphyrin **3** can be regenerated upon application of 0 V, indicating a stable cationic species.

Upon the one-electron reduction of dithiaporphyrin **3** to its radical anion (Figure 3b), a large decrease in Soret band intensity is observed flanked by two small features that grow in at 383 and 474 nm. Upon reduction, Q-bands I, II, and IV show decreases in intensity concomitant with intensity increases of two broad features at 600 and 850 nm and a small peak at 750 nm. The inset of Figure 3b shows an expansion of the Q-band region and the neutral spectrum of **3** appears to have a peak ∼820 nm, which is an experimental artifact due to the diameter of wires used in the Pt mesh electrode. Nevertheless, upon reduction there is clear evidence for an increase in absorption ∼850 nm, which then returns to baseline at ∼930 nm. Again, the neutral absorption spectrum of **3** can be regenerated by applying 0 V to the cell.

Both the cationic and anionic absorption spectra show red-shifted features compared to the neutral dithiaporphyrin **3**. There is a wealth of literature that has examined the

dx.doi.org/10.1021/jo302707f | J. Org. Chem. 2013, 78, 1612−1620

Table 3. DFT Calculations and Molecular Orbital Energies for Cationic, Anionic and Neutral 3 and 4 Obtained at the B3LYP/6-31G+(d) Level

calcd MO energies	3 (eV)	4 (eV)	3^+ (eV)	4^+ (eV)	3^- (eV)	4^- (eV)
LUMO+1	−2.78	−2.82	−5.53	−5.60	+0.43	+0.31
LUMO	−2.85	−2.91	−5.70	−5.77	−0.15	−0.24
HOMO	−5.36	−5.42	−7.93[a]	−7.99[a]	−1.09[a]	−1.17[a]
HOMO-1	−5.71	−5.77	−8.36	−8.43	−2.81	−2.88
HOMO-2	−6.34	−6.38	−8.78	−8.84	−3.17	−3.24

[a]SOMO orbital.

spectroelectrochemical features of H_2TPP[51−56] and limited reports on dithiaporphyrins.[32] There are many similarities in the spectral features between the porphyrins and dithiaporphyrins, and we have borrowed several of the ideas presented in the H_2TPP literature to explain similar phenomena in the dithiaporphyrins. For example, the absorption spectrum of diprotonated porphyrins (H_4TPP^{2+}) is very similar to the electrochemically generated radical cation absorption spectrum.[41] Similarly, the diprotonated dithiaporphyrin absorption spectrum[32] is similar to the radical cation spectrum. Drawing conclusions pertaining to the structure of the porphyrin and its absorption spectrum is difficult, as there are no crystal structures of a radical cation porphyrin. However, the crystal structure of H_4TPP^{2+} was solved[57] and shows a large deviation in the macrocyclic aromatic core accompanied by a twist of the four *meso*-phenyl groups to become more planar[40] with the methine *meso*-positions.[37] We propose that the electrochemically generated radical cation of **3** exhibits a significant deformation of the macrocyclic plane, and thus a break in the FMO degeneracy, leading to the observed spectral features shown in Figure 3. Beyond the break in orbital degeneracy, it is postulated that oxidation of the dithiaporphyrin cores result in a decrease in the S···S interaction, which holds the transannular heteroatoms close, resulting in deforming the macrocyclic aromatic plane of the neutral dithiaporphyrin. More discussion on the structural features of the cation and anion is presented in the calculations section. The reversibility of these redox species implies that the compounds could address longevity issues associated with organic materials applications.

DFT Calculations. Optimized geometries of reduced model compounds generated by replacing alkyl fragments on *meso*-phenyl substituents with methyl groups for porphyrins **3** and **4** were calculated using DFT methods at the B3LYP/6-31G+(d) level with the Gaussian09 suite of programs.[58] The DFT-calculated structures match reasonably well with the six crystal structures of dithiaporphyrins[42,59−62] in the Cambridge Crystallographic Data Centre (updated February 2012), especially considering the transannular S···S distance in the calculated structures was 3.07 Å. The crystallographically determined structure of TP-N_2S_2[42] was overlaid with the calculated structure by removing the *p*-phenyl groups and replacing them with hydrogen, and the resulting overlay (Figure S14 in the Supporting Information) shows an average root-mean-square deviation of 0.11 Å with a maximum deviation of 0.28 Å as determined by Mercury 3.0 CSD,[63] which strongly supports the basis set selection for the ground-state geometry. The most significant structural difference arises from the pyrrolic rings being out of macrocyclic plane by 0.16 Å in the crystal structure, whereas the calculated structure shows the pyrrolic rings coplanar with the macrocyclic ring.

The calculated FMO energies for **3** and **4** and both the radical cations and anions data are compiled in Table 3. Figure 4 illustrates the FMO energy levels and depicts the HOMO and LUMO Kohn−Sham orbital shapes for dithiaporphyrin **4** (**3** is

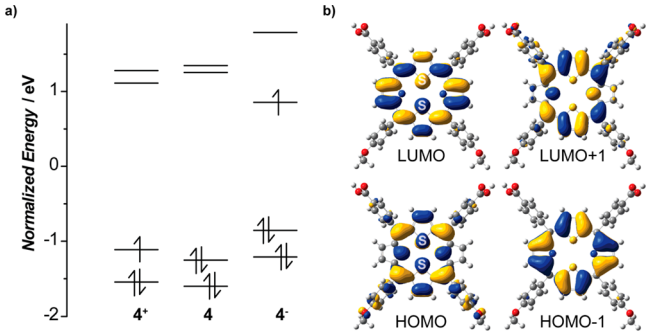

Figure 4. (a) Normalized energies of cationic, neutral and anionic dithiaporphyrin **4** and (b) frontier molecular orbitals of neutral porphyrin **4** using DFT methods at the B3LYP/6-31G+(d) level.

indistinguishable and included in Figure S10 the Supporting Information). The 18 π-electron aromatic core sits nearly planar and the *meso*-substituted phenyl rings are at dihedral angles of 65° to the macrocyclic core, which compares well with calculated structures of tetrapyrrolic porphyrin analogues.[64] DFT calculations do reveal a break in the degeneracy of the two highest occupied MOs resulting from a change in symmetry by the incorporation of thiophene into the core. Interestingly, compared to our previously synthesized dithiaporphyrins,[32] the HOMO energies of **3** and **4** have remained relatively unchanged while the LUMO energies have decreased from about −3.2 to −2.8 eV, resulting in a smaller HOMO−LUMO energy gap overall, which is attributed to the addition of the electron-withdrawing diester groups. Furthermore, Figure S13 in the Supporting Information shows significant overlap of electron density between the trans-annular sulfurs in HOMO-6, leading to the nearly planar macrocycle and the ambipolar electrochemical behavior.

The DFT-calculated HOMO−LUMO gap is 2.51 eV for both dithiaporphyrins **3** and **4**, which corresponds to an optical transition at 494 nm, clearly a large overestimation of the experimental energy gap at 706 nm (1.75 eV). The failure of TD-DFT calculations based on the B3LYP functional to examine porphyrin charge-transfer excited states has been documented previously[65] and dithiaporphyrins seem to suffer the same limitation. Note that long-range corrected (LC) functionals were assessed, as deployed in Gaussian09, and did not result in appreciable differences in the FMOs. The DFT-calculated E_{HOMO} of −5.4 eV matches the electrochemically derived data and the E_{LUMO} was calculated to be −2.9 eV, which is slightly higher than the experimentally estimated value of −3.4 eV by cyclic voltammetry. These discrepancies are most likely attributed to limitations in DFT methods used and lack of

dx.doi.org/10.1021/jo302707f | J. Org. Chem. 2013, 78, 1612−1620

solvent parameters.[65] The calculated MO energies for **3** and **4** are very similar, which is consistent with their nearly identical optical and electrochemical data. Normalized FMO energies of **4**, its radical cation $4^{\bullet+}$ and its radical anion $4^{\bullet-}$ are shown in Figure 4. Note that a normalized energy scale was used by setting the Fermi level, $^1/_2(E_{LUMO}-E_{HOMO})$, of the neutral dithiaporphyrin at 0 eV. The complete FMO energies of cationic, anionic and neutral **3** and **4** are summarized in Figures S11 and S12 in the Supporting Information. The optimized structures of the radical cations and anions provide insight into the spectroelectrochemical features observed in Figure 3. First, the optimized radical cation structure shows significant deviations in planarity of the macrocycle from the neutral nearly planar dithiaporphyrin. The pyrrolic rings remain in plane and the thiophene sulfurs are 0.28 and 0.41 Å out of the macrocycle plane, disrupting conjugation. Furthermore, to stabilize the cationic charge, the two alkoxyphenyl *meso*-substituents have rotated into conjugation with dihedral angles of 49.5° compared to 65° in the neutral dithiaporphyrin. The two diester substituted *meso*-phenyl substituents are nearly unchanged with dihedral angles of 64°. The net result is an extension of conjugation though the *meso*-position and weakened conjugation in the macrocyclic core leading to an overall modest red-shift in the absorption properties, as shown in Figure 3a. Second, the optimized radical anion structure shows a nearly planar macrocyclic structure with sulfurs deviating from the macrocyclic plane by only 0.14 and 0.17 Å, which is similar to the calculated neutral dithiaporphyrin. Similarly to the cation, the *meso*-phenyl substituents show a change compared to the neutral dithiaporphyrin. The electron deficient *meso*-phenyl esters show dihedral angles of 49.5°, and the alkoxyphenyl *meso*-substituents show dihedral angles of 60.6° relative to the macrocyclic core. Clearly, the rotations of the *meso*-phenyl groups play a role in stabilizing the anionic charge on the macrocyclic ring. The net results of these stabilizations are an extension of the aromatic character beyond the macrocyclic core leading a significant red-shifted absorbance as observed in Figure 3b for the radical anion.

CONCLUSION

In summary, two 21,23-dithiaporphyrins have been synthesized that exhibit absorbance profiles with high molar absorptivities over a wide wavelength range. The redox properties show that these dithiaporphyrins are reversibly reduced and oxidized at modest potentials. DFT calculations confirm that the electronics of both dithiaporphyrins are similar and have been electronically tuned to possess a smaller HOMO−LUMO energy gap compared to tetraphenylporphyrins. Furthermore, spectroelectrochemical experiments confirm the reversible conversion to either the radical anion or radical cation, and the combination of reversible redox properties with a small HOMO−LUMO energy difference suggests these dithiaporphyrins could behave as ambipolar materials for organic electronic devices.

EXPERIMENTAL SECTION

Column chromatography was performed on P60 silica gel (230−400 mesh). Thin-layer chromatography was carried out on silica gel F-254 glass-backed TLC plates. Solvents were used as received or dried using a solvent purification system and reactions were performed under ambient atmosphere unless otherwise stated.

NMR spectra were recorded on either a 300 or 400 MHz spectrometer. ^{1}H and ^{13}C NMR assignments were assisted by 2D gHSQC and gCOSY NMR spectra on a 600 MHz spectrometer at 330 K. Residual solvent peaks were as follows: chloroform, δ 7.26 ppm; ethyl acetate, δ 2.05, 4.12 1.26 ppm; *N*,*N*-dimethylformamide, δ 8.02, 3.30, 2.96, 2.88 ppm. Accurate mass spectra were recorded using either ESI or MALDI-TOF techniques. UV−vis spectra were recorded using a spectrophotometer in dual beam mode. Cyclic voltammetry (CV) experiments were carried out on a potentiostat that was controlled by a PC in a temperature controlled, three-electrode cell (15 mL). The working electrode was a glassy carbon disc with area of 0.28 cm^2, which was polished after each use with 0.05 μm diamond slurry in an automated polisher. The reference electrode was a Ag wire and the counter electrode was a Pt wire that was flame annealed prior to each use. All potentials were referenced to the ferrocene/ferrocenium redox couple. Each CV experiment consisted of approximately 1−3 mM redox active species dissolved in 0.1 M tetrabutylammonium hexafluorophosphate in deoxygenated methylene chloride, by bubbling with Ar for 10 min prior to dissolving the redox active species and an Ar blanket was maintained during the experiment. Spectroelectrochemical spectra were generated with a spectrophotometer linked with a potentiostat using an optically transparent thin layer electrochemical (OTTLE) cell.[50] The working electrode in the beam path was a Pt mesh, the counter electrode was another Pt mesh, and a silver wire acted as a pseudoreference electrode using the same solvent and electrolyte as above.

Butyl 4-Formylbenzoate. 4-Formylbenzoic acid (1.0 g, 6.7 mmol), KI (1.1 g, 6.7 mmol), and K_2CO_3 (0.9 g, 13.4 mmol) were dissolved in DMF (15 mL) and heated to 100 °C for 2 h. To the hot solution was added 1-bromobutane (0.9 mL, 8.1 mmol), the resulting yellow solution was left at 100 °C for an additional 12 h, and then DMF was removed under reduced pressure. The residue was dissolved in $CHCl_3$ (50 mL), washed with water (100 mL) and saturated $NaHCO_3$ (50 mL), and then dried with Na_2SO_4. The crude yellow oil was purified by column chromatography using hexanes and ethyl acetate (4.5:0.5) to afford a clear oil (1.2 g, 90%): ^{1}H NMR (400 MHz, $CDCl_3$) δ 10.10 (s, 1H, C*H*O), 8.19 (d, J = 8.4 Hz, 2H, aryl), 7.94 (d, J = 8.2 Hz, 2H, aryl), 4.36 (t, J = 6.6 Hz, 2H, (C═O)OCH_2), 1.86−1.65 (m, 2H, (C═O)OCH$_2$CH_2), 1.58−1.40 (m, 2H, (C═O)OCH$_2$CH$_2$CH_2), 0.99 (t, J = 7.4 Hz, 3H, CH_3); ^{13}C NMR (101 MHz, $CDCl_3$) δ 191.7, 165.8, 139.3, 135.7, 130.3, 129.6, 65.6, 30.8, 19.4, 13.9. Spectroscopic data are consistent with the reported synthesis by Abreu and co-workers.[33]

4-(Dodecyloxy)benzaldehyde. 4-Hydroxybenzaldehyde (3.66 g, 30.0 mmol), KI (4.98 g, 30.0 mmol), and K_2CO_3 (8.28 g, 60.0 mmol) were added to acetone (70 mL) and refluxed for 2 h. To the hot solution was added slowly 1-bromododecane (7.9 mL, 33 mmol) and the solution refluxed for 24 h. Acetone was then removed under reduced pressure, and the residue was suspended in water (100 mL), extracted with dichloromethane, and washed with NaOH (150 mL, 2%). The organic layer was dried with Na_2SO_4, and the solvent was removed under reduced pressure to afford the crude product. The crude mixture was subjected to silica gel column chromatography using a mixture of hexanes and ethyl acetate (4.5:0.5) to afford the pure compound as an off-white oil (5.77 g, 67%): ^{1}H NMR (400 MHz, $CDCl_3$) δ 9.84 (s, 1H, Ar-C*H*O), 7.78 (d, J = 8.8 Hz, 2H, aryl), 6.95 (d, J = 8.7 Hz, 2H, aryl), 3.99 (t, J = 6.6 Hz, 2H, Ar-OCH_2), 1.82−1.74 (m, 2H, Ar-OCH$_2$CH_2), 1.48−1.39 (m, 2H, Ar-OCH$_2$CH$_2$CH_2), 1.33−1.21 (m, 16H, aliphatic), 0.86 (t, J = 6.8 Hz, 3H, CH_3); ^{13}C NMR (101 MHz, $CDCl_3$) δ 190.7, 164.3, 132.0, 129.8, 114.77, 68.4, 32.0, 29.7, 29.7, 29.6, 29.6, 29.4, 29.1, 26.0, 22.7, 14.2. Spectroscopic data are consistent with the reported synthesis by Bromby and co-workers.[32]

2,5-Bis[(4-butoxycarbonylphenyl)hydroxymethyl]thiophene (1a). To a solution of hexanes (30 mL) were added *n*-BuLi (5.2 mL of 2.3 M solution in hexane, 12 mmol) and distilled TMEDA (1.8 mL, 12 mmol) and the mixture stirred under nitrogen. Thiophene (0.44 mL, 5.5 mmol) was added, and the solution was refluxed for 1 h. The dilithiated thiophene was cooled to room temperature and then transferred to a 0 °C solution of butyl 4-formylbenzoate (2.44 g, 12 mmol). The reaction was quenched with water (30 mL) and the aqueous layer was extracted with diethyl ether (100 mL). The organic

dx.doi.org/10.1021/jo302707f | J. Org. Chem. 2013, 78, 1612−1620

layer was dried with Na_2SO_4, and the solvent was removed under reduced pressure to afford the crude product. Silica gel column chromatography using hexanes and ethyl acetate (4:1) afforded a pure yellow oil **1a** (1.7 g, 63%): ^{1}H NMR (400 MHz, $CDCl_3$) δ 7.96 (d, J = 8.3 Hz, 2H, aryl), 7.44 (d, J = 6.7 Hz, 2H, aryl), 6.66 (s, 1H, C*H*OH), 5.95 (s, 1H, β-thiophene), 4.28 (t, J = 6.6 Hz, 2H, (C═O)OCH_2), 1.82−1.64 (m, 2H, (C═O)OCH$_2$CH_2), 1.55−1.37 (m, 2H, (C═O)OCH$_2$CH$_2$CH_2), 0.97 (t, J = 7.4 Hz, 3H, CH_3); ^{13}C NMR (101 MHz, $CDCl_3$) δ 166.6, 148.0, 147.9, 147.8, 129.9, 126.2, 124.8, 72.0, 65.1, 30.8, 19.4, 13.9; HR-MS (ESI) calcd for $C_{28}H_{32}SO_6Na$ (M + Na)$^+$ 519.1812, found 519.1800.

2,5-Bis[(4-dodecyloxyphenyl)hydroxymethyl]thiophene (1b). To a solution of hexanes (30 mL) were added *n*-BuLi (3.9 mL of 1.4 M solution in hexane, 5.5 mmol) and distilled TMEDA (0.8 mL, 5.4 mmol) and the mixture stirred under nitrogen atmosphere. Thiophene (0.18 mL, 2.2 mmol) was added, and the solution was refluxed for 1 h. The dilithiated thiophene was cooled to room temperature and then transferred to a 0 °C solution of 4-(dodecyloxy)benzaldehyde (1.58 g, 5.4 mmol). The reaction was quenched with water (30 mL), and the aqueous layer was extracted with diethyl ether (100 mL). The organic layer was dried with Na_2SO_4, and the solvent was removed under reduced pressure to afford the crude product. Silica gel column chromatography using hexanes and ethyl acetate (4:1) afforded a pure yellow oil **1b** (0.32 g, 22%): ^{1}H NMR (400 MHz, $CDCl_3$) δ 7.32 (d, J = 8.5 Hz, 2H, aryl), 6.86 (d, J = 8.6 Hz, 2H, aryl), 6.68 (d, J = 2.7 Hz, 1H, C*H*OH), 5.90 (s, 1H, β-thiophene), 3.94 (t, J = 6.6 Hz, 2H, ArOCH_2), 2.38 (s, 1H), 1.85−1.68 (m, 2H, ArOCH$_2$CH_2), 1.55−1.38 (m, 2H, ArOCH$_2$CH$_2$CH_2), 1.29−1.21 (m, 16H, aliphatic), 0.89 (t, J = 6.8 Hz, 3H, CH_3); ^{13}C NMR (101 MHz, $CDCl_3$) δ 159.1, 148.5, 135.1, 127.7, 124.3, 114.6, 72.4, 68.2, 32.1, 29.8, 29.8, 29.8, 29.7, 29.6, 29.5, 29.4, 26.2, 22.8, 14.3; HR-MS (ESI) calcd for $C_{42}H_{63}O_3S$ (M − OH)$^+$ 647.4493, found 647.4492.

5,10-Bis(4-butoxycarbonylphenyl)-16-thiatripyrrane (2a). Dialcohol **1a** (180 mg, 0.4 mmol) was added to freshly distilled pyrrole (5 mL, 72 mmol) and purged with N_2 for 10 min. The solution was foil wrapped, and 1 drop of BF_3·OEt_2 (~0.2 mL, 1.63 mmol) was added resulting in an immediate dark solution. After the solution was stirred for 48 h, NaOH (30 mL, 40%) was added and the solution extracted with methylene chloride (100 mL) and dried with Na_2SO_4. The solvent was evaporated under reduced pressure, and the remaining pyrrole was recovered by distillation. The crude brown oil was purified by column chromatography using hexanes and ethyl acetate (3.5:1.5) to afford the pure compound as a brown-pink oil **2a** (86 mg, 40%): ^{1}H NMR (300 MHz, $CDCl_3$) δ 7.98 (d, J = 8.2 Hz, 2H, aryl), 7.30 (d, J = 8.1 Hz, 2H, aryl), 6.71 (s, 1H, α-pyrrole), 6.62 (s, 1H, β-thiophene), 6.14 (dd, J = 5.6, 2.7 Hz, 1H, β-pyrrole), 5.90 (s, 1H, β-pyrrole), 5.61 (s, 1H, meso-C*H*), 4.31 (t, J = 6.6 Hz, 2H, (C═O)OCH_2), 1.82−1.66 (m, 2H, (C═O)OCH$_2$CH_2), 1.55−1.37 (m, 2H, (C═O)OCH$_2$CH$_2$CH_2), 0.98 (t, J = 7.3 Hz, 3H, CH_3); ^{13}C NMR (75 MHz, $CDCl_3$) δ 166.6, 147.7, 145.4, 132.2, 130.0, 129.5, 128.5, 125.8, 117.8, 108.6, 108.0, 65.0, 46.1, 30.9, 19.4, 13.9; HR-MS (MALDI-TOF) calcd for $C_{36}H_{38}N_2O_4SNa$ (M + Na)$^+$ 617.2444, found 617.2429.

5,10-Bis(4-dodecyloxyphenyl)-16-thiatripyrrane (2b). Dicarbinol **1b** (0.31 g, 0.5 mmol) was added to freshly distilled pyrrole (5 mL, 72 mmol) and purged with N_2 for 10 min. The solution was foil wrapped, and 1 drop of BF_3·OEt_2 (~0.2 mL, 1.63 mmol) was added resulting in an immediate dark solution. After the solution was stirred for 1 h, NaOH (30 mL, 40%) was added and the solution extracted with methylene chloride (100 mL) and dried with Na_2SO_4. The solvent was evaporated under reduced pressure, and the remaining pyrrole was recovered by distillation. The crude brown oil was purified by column chromatography using hexanes and ethyl acetate (4:1) to afford the pure compound as a green-brown oil **2b** (0.36 g, 93%): ^{1}H NMR (400 MHz, $CDCl_3$) δ 7.87 (s, 1H, N*H*), 7.14 (d, J = 8.6 Hz, 2H, aryl), 6.83 (d, J = 8.6 Hz, 2H, aryl), 6.68 (s, 1H, α-pyrrole), 6.60 (s, 1H, β-thiophene), 6.14 (s, 1H, β-pyrrole), 5.92 (s, 1H, β-pyrrole), 5.51 (s, 1H, meso-C*H*), 3.94 (t, J = 6.5 Hz, 2H, PhO-CH_2), 1.84−1.73 (m, 2H, PhOCH$_2$CH_2), 1.52−1.41 (m, 2H, PhOCH$_2$CH$_2$CH_2), 1.39−1.23 (m, 16H, aliphatic), 0.90 (t, J = 6.8 Hz, 3H, CH_3); ^{13}C NMR (101 MHz, $CDCl_3$) δ 158.3, 146.4, 134.8, 133.6, 129.5, 125.2, 117.2, 114.6, 108.4, 107.5, 68.1, 66.0, 45.4, 32.1, 31.7, 29.8, 29.8, 29.6, 29.5, 29.5, 26.2, 22.8, 14.2; HR-MS (MALDI-TOF) calcd for $C_{50}H_{70}N_2SO_2Na$ (M + Na)$^+$ 785.5050, found 785.5015.

5, 10-Bis(4-butoxycarbonylphenyl)-15,20-bis(4-dodecyloxyphenyl)-21,23-dithiaporphyrin (3). Thiatripyrrane **2a** (0.54 g, 0.9 mmol) and dicarbinol **1b** (0.61 g, 0.9 mmol) were dissolved in methylene chloride and degassed with N_2 for 15 min. The solution was foil wrapped, BF_3·OEt_2 (0.06 mL, 0.5 mmol) was added, and the solution immediately turned dark. After the solution was stirred for 2 h, DDQ (0.20 g, 0.9 mmol) was added, and the solution was stirred in air for an additional 3 h. The solution was passed through a short alumina column using methylene chloride as the eluent. After removal of solvent under reduced pressure, a black-purple crude compound was obtained. Column chromatography was used using methylene chloride and hexanes (4:1) to afford pure purple crystals of **3** (173 mg, 16%): ^{1}H NMR (300 MHz, $CDCl_3$) δ 9.83 (s, 1H, β-thiophene), 9.73 (s, 1H, β-thiophene), 8.82 (d, J = 4.6 Hz, 1H, β-pyrrole), 8.72 (d, J = 4.6 Hz, 1H, β-pyrrole), 8.59 (d, J = 8.3 Hz, 2H, aryl), 8.42 (d, J = 8.3 Hz, 2H, aryl), 8.20 (d, J = 8.6 Hz, 2H, aryl), 7.36 (d, J = 8.6 Hz, 2H, aryl), 4.62 (t, J = 6.6 Hz, 2H, (C═O)OCH_2), 4.23 (t, J = 6.5 Hz, 2H, O−CH_2), 2.08−1.92 (m, 4H, aliphatic), 1.81−1.62 (m, 4H, aliphatic), 1.62−1.29 (m, 16H, aliphatic), 1.18 (t, J = 7.4 Hz, 3H, CH_3), 1.01 (t, J = 6.6 Hz, 3H, CH_3); ^{13}C NMR (75 MHz, $CHCl_3$) δ 166.8, 159.5, 156.9, 156.0, 148.6, 147.2, 145.9, 135.9, 135.5, 135.1, 134.9, 134.2, 134.1, 133.2, 132.4, 130.3, 128.7, 113.7, 104.6, 68.3, 65.3, 32.1, 31.0, 30.9, 29.8, 29.8, 29.6, 29.5, 26.3, 22.8, 19.5, 19.4, 14.2, 14.0, 13.8; HR-MS (MALDI-TOF) calcd for $C_{78}H_{93}N_2O_6S_2$ (M + H)$^+$ 1217.6470, found 1217.6468.

5, 10-Bis(4-carboxyphenyl)-15,20-bis(4-dodecyloxyphenyl)-21,23-dithiaporphyrin (4). Dithiaporphyrin **3** (173 mg, 0.14 mmol) and LiOH (0.6 g, 25 mmol) were added to THF and water (20 mL, 1:1) and the solution heated to 70 °C and stirred for 24 h. The solution was acidified to ~pH 4 with concd HCl followed by removal of THF under reduced pressure. The precipitate was filtered to afford purple crystals of **4** (151 mg, 98%) which were not further purified: ^{1}H NMR (600 MHz, DMF) δ 9.86 (s, 1H), 9.79 (s, 1H), 8.76 (d, J = 4.4 Hz, 1H), 8.71 (d, J = 4.4 Hz, 1H), 8.56 (d, J = 8.2 Hz, 2H), 8.45 (d, J = 7.9 Hz, 2H), 8.26 (d, J = 8.5 Hz, 2H), 7.52 (d, J = 8.6 Hz, 2H), 4.37 (t, J = 6.4 Hz, 3H), 2.07−1.94 (m, 3H), 1.67 (m, 2H), 1.56−1.47 (m, 2H), 1.47−1.30 (m, 14H), 0.91 (t, J = 7.1 Hz, 3H); ^{13}C NMR (151 MHz, DMF) δ 169.0, 160.9, 157.7, 157.1, 149.4, 148.4, 145.9, 145.1, 137.0, 136.8, 136.6, 136.0, 135.9, 135.2, 135.2, 134.1, 134.1, 129.8, 115.2; ^{13}C DEPT 135 NMR (151 MHz, DMF) 68.5, 31.8, 29.6, 29.6, 29.5, 29.4, 29.4, 29.2, 26.1, 22.5; HR-MS (MALDI-TOF) calcd for $C_{70}H_{77}N_2O_6S_2$ (M + H)$^+$ 1105.5218, found 1105.5242.

■ ASSOCIATED CONTENT

Supporting Information

^{1}H and ^{13}C NMR spectra; absorption and emission properties and spectra of **3** and **4**; cyclic voltammograms, diffusion coefficients, and electron-transfer rates of **3** and **4**; DFT calculations and summarized energies of **3** and **4**; crystallographic data overlaid with calculated structure. Cartesian coordinates of DFT-calculated structures. This material is available free of charge via the Internet at http://pubs.acs.org.

■ AUTHOR INFORMATION

Corresponding Author

*Tel: +1 403 220 7559. Fax: +1 403 289 9488. E-mail: todd.sutherland@ucalgary.ca.

Notes

The authors declare no competing financial interest.

■ ACKNOWLEDGMENTS

A.D.B. thanks Dr. A. Scott Hinman for helpful discussions, Douglas Brown for fluorescence assistance, and the Government of Alberta for a scholarship. We thank the Canada School of Energy for a proof-of-principle grant and NSERC of Canada Discovery Grant to carry out this work. The computational research has been enabled by the use of computing resources provided by WestGrid and Compute/Calcul Canada.

■ REFERENCES

(1) Wong, W. W. H.; Vak, D.; Singh, T. B.; Ren, S.; Yan, C.; Jones, D. J.; Liaw, I. I.; Lamb, R. N.; Holmes, A. B. *Org. Lett.* **2010**, *12*, 5000−5003.
(2) Li, W.; Lee, T.; Oh, S. J.; Kagan, C. R. *ACS Appl. Mater. Interfaces* **2011**, *3*, 3874−3883.
(3) Opitz, A.; Bronner, M.; Brütting, W.; Himmerlich, M.; Schaefer, J. A.; Krischok, S. *Appl. Phys. Lett.* **2007**, *90*, 212112.
(4) Chesterfield, R. J.; Newman, C. R.; Pappenfus, T. M.; Ewbank, P. C.; Haukaas, M. H.; Mann, K. R.; Miller, L. L.; Frisbie, C. D. *Adv. Mater.* **2003**, *15*, 1278−1282.
(5) Anthony, J. E.; Facchetti, A.; Heeney, M.; Marder, S. R.; Zhan, X. *Adv. Mater.* **2010**, *22*, 3876−3892.
(6) Facchetti, A. *Chem. Mater.* **2011**, *23*, 733−758.
(7) Figueira-Duarte, T. M.; Muellen, K. *Chem. Rev.* **2011**, *111*, 7260−7314.
(8) Pron, A.; Gawrys, P.; Zagorska, M.; Djurado, D.; Demadrille, R. *Chem. Soc. Rev.* **2010**, *39*, 2577−2632.
(9) Zhan, X.; Facchetti, A.; Barlow, S.; Marks, T. J.; Ratner, M. A.; Wasielewski, M. R.; Marder, S. R. *Adv. Mater.* **2011**, *23*, 268−284.
(10) Zhao, X.; Zhan, X. *Chem. Soc. Rev.* **2011**, *40*, 3728−3743.
(11) Cravino, A. *Polym. Int.* **2007**, *56*, 943−956.
(12) Tsuji, H.; Mitsui, C.; Sato, Y.; Nakamura, E. *Adv. Mater.* **2009**, *21*, 3776−3779.
(13) Chen, C.-H.; Huang, W.-S.; Lai, M.-Y.; Tsao, W.-C.; Lin, J. T.; Wu, Y.-H.; Ke, T.-H.; Chen, L.-Y.; Wu, C.-C. *Adv. Funct. Mater.* **2009**, *19*, 2661−2670.
(14) Camaioni, N.; Tinti, F.; Degli Esposti, A.; Righi, S.; Usluer, O. z.; Boudiba, S.; Egbe, D. A. M. *Appl. Phys. Lett.* **2012**, *101*, 053302.
(15) Cornil, J.; Bredas, J.-L.; Zaumseil, J.; Sirringhaus, H. *Adv. Mater.* **2007**, *19*, 1791−1799.
(16) Feng, X.; Liu, L.; Honsho, Y.; Saeki, A.; Seki, S.; Irle, S.; Dong, Y.; Nagai, A.; Jiang, D. *Angew. Chem., Int. Ed.* **2012**, *51*, 2618−2622.
(17) Hayashi, H.; Nihashi, W.; Umeyama, T.; Matano, Y.; Seki, S.; Shimizu, Y.; Imahori, H. *J. Am. Chem. Soc.* **2011**, *133*, 10736−10739.
(18) Khademi, S.; Song, J. Y.; Wyatt, P. B.; Kreouzis, T.; Gillin, W. P. *Adv. Mater.* **2012**, *24*, 2278−2283.
(19) Kulkarni, A. P.; Zhu, Y.; Babel, A.; Wu, P.-T.; Jenekhe, S. A. *Chem. Mater.* **2008**, *20*, 4212−4223.
(20) Wong, W. W. H.; Vak, D.; Singh, T. B.; Ren, S.; Yan, C.; Jones, D. J.; Liaw, I. I.; Lamb, R. N.; Holmes, A. B. *Org. Lett.* **2010**, *12*, 5000−5003.
(21) Yella, A.; Lee, H.-W.; Tsao, H. N.; Yi, C.; Chandiran, A. K.; Nazeeruddin, M. K.; Diau, E. W.-G.; Yeh, C.-Y.; Zakeeruddin, S. M.; Grätzel, M. *Science* **2011**, *334*, 629−634.
(22) Hizume, Y.; Tashiro, K.; Charvet, R.; Yamamoto, Y.; Saeki, A.; Seki, S.; Aida, T. *J. Am. Chem. Soc.* **2010**, *132*, 6628−6629.
(23) Kwong, R. C.; Sibley, S.; Dubovoy, T.; Baldo, M.; Forrest, S. R.; Thompson, M. E. *Chem. Mater.* **1999**, *11*, 3709−3713.
(24) Wan, S.; Gandara, F.; Asano, A.; Furukawa, H.; Saeki, A.; Dey, S. K.; Liao, L.; Ambrogio, M. W.; Botros, Y. Y.; Duan, X.-F.; Seki, S.; Stoddart, J. F.; Yaghi, O. M. *Chem. Mater.* **2011**, *23*, 4094−4097.
(25) Warman, J. M.; de, H. M. P.; Dicker, G.; Grozema, F. C.; Piris, J.; Debije, M. G. *Chem. Mater.* **2004**, *16*, 4600−4609.
(26) Che, C.-M.; Xiang, H.-F.; Chui, S. S.-Y.; Xu, Z.-X.; Roy, V. A. L.; Yan, J. J.; Fu, W.-F.; Lai, P. T.; Williams, I. D. *Chem.—Asian J.* **2008**, *3*, 1092−1103.
(27) So, M.-H.; Roy, V. A. L.; Xu, Z.-X.; Chui, S. S.-Y.; Yuen, M.-Y.; Ho, C.-M.; Che, C.-M. *Chem.—Asian J.* **2008**, *3*, 1968−1978.
(28) Grozema, F. C.; Houarner-Rassin, C.; Prins, P.; Siebbeles, L. D. A.; Anderson, H. L. *J. Am. Chem. Soc.* **2007**, *129*, 13370−13371.
(29) Yuan, Y.; Gregg, B. A.; Lawrence, M. F. *J. Mater. Res.* **2000**, *15*, 2494−2498.
(30) Warman, J. M.; Van, D. C. A. M. *Mol. Cryst. Liq. Cryst.* **2003**, *396*, 41−72.
(31) Schouten, P. G.; Warman, J. M.; De, H. M. P.; Fox, M. A.; Pan, H. L. *Nature* **1991**, *353*, 736−7.
(32) Bromby, A. D.; Kan, W. H.; Sutherland, T. C. *J. Mater. Chem.* **2012**, *22*, 20611−20617.
(33) Abreu, M. F.; Salvador, V. T.; Vitorazi, L.; Gatts, C. E. N.; dos Santos, D. R.; Giacomini, R.; Cardoso, S. L.; Miranda, P. C. M. L. *Carbohydr. Res.* **2012**, *353*, 69−78.
(34) Bhat, A. R.; Bhat, A. I.; Athar, F.; Azam, A. *Helv. Chim. Acta* **2009**, *92*, 1644−1656.
(35) Punidha, S.; Agarwal, N.; Ravikanth, M. *Eur. J. Org. Chem.* **2005**, *2005*, 2500−2517.
(36) Krüger, R. A.; Terpstra, A. S.; Sutherland, T. C. *Can. J. Chem.* **2011**, *89*, 214−220.
(37) Ulman, A.; Manassen, J. *J. Am. Chem. Soc.* **1975**, *97*, 6540−6544.
(38) Fajer, J.; Borg, D. C.; Forman, A.; Dolphin, D.; Felton, R. H. *J. Am. Chem. Soc.* **1970**, *92*, 3451−3459.
(39) Tao, M.; Zhou, X.; Jing, M.; Liu, D.; Xing, J. *Dyes Pigm.* **2007**, *75*, 408−412.
(40) Ulman, A.; Manassen, J.; Frolow, F.; Rabinovich, D. *Inorg. Chem.* **1981**, *20*, 1987−1990.
(41) Hill, R. L.; Gouterman, M.; Ulman, A. *Inorg. Chem.* **1982**, *21*, 1450−1455.
(42) Latos-Grazynski, L.; Lisowski, J.; Szterenberg, L.; Olmstead, M. M.; Balch, A. L. *J. Org. Chem.* **1991**, *56*, 4043−4045.
(43) Nicholson, R. S. *Anal. Chem.* **1965**, *37*, 1351−1355.
(44) Hinman, A. S.; Pavelich, B. J.; Kondo, A. E.; Pons, S. *J. Electroanal. Chem. Interfacial Elechochem.* **1987**, *234*, 145−162.
(45) Dolphin, D.; Felton, R. H.; Borg, D. C.; Fajer, J. *J. Am. Chem. Soc.* **1970**, *92*, 743−745.
(46) Kadish, K. M.; Rhodes, R. K. *Inorg. Chem.* **1981**, *20*, 2961−2966.
(47) Guzinski, J. A.; Felton, R. H. *J. Chem. Soc., Chem. Commun.* **1973**, 715−716.
(48) Scharber, M. C.; Mühlbacher, D.; Koppe, M.; Denk, P.; Waldauf, C.; Heeger, A. J.; Brabec, C. J. *Adv. Mater.* **2006**, *18*, 789−794.
(49) Gomer, R.; Tryson, G. *J. Chem. Phys.* **1977**, *66*, 4413−4424.
(50) Krejčik, M.; Daněk, M.; Hartl, F. *J. Electroanal. Chem. Interfacial Elechochem.* **1991**, *317*, 179−187.
(51) D'Souza, F.; Villard, A.; Van, C. E.; Franzen, M.; Boschi, T.; Tagliatesta, P.; Kadish, K. M. *Inorg. Chem.* **1993**, *32*, 4042−8.
(52) Kadish, K. M.; Rhodes, R. K. *Inorg. Chem.* **1981**, *20*, 2961−6.
(53) Lin, C.-l.; Fang, M.-Y.; Cheng, S.-H. *J. Electroanal. Chem.* **2002**, *531*, 155−162.
(54) Moore, K. T.; Fletcher, J. T.; Therien, M. J. *J. Am. Chem. Soc.* **1999**, *121*, 5196−5209.
(55) Postlethwaite, T. A.; Hutchison, J. E.; Hathcock, K. W.; Murray, R. W. *Langmuir* **1995**, *11*, 4109−16.
(56) Tagliatesta, P.; Li, J.; Autret, M.; Van, C. E.; Villard, A.; D'Souza, F.; Kadish, K. M. *Inorg. Chem.* **1996**, *35*, 5570−5576.
(57) Stone, A.; Fleischer, E. B. *J. Am. Chem. Soc.* **1968**, *90*, 2735−2748.
(58) Gaussian 09, Revision C.01: Frisch, M. J.; Trucks, G. W.; Schlegel, H. B.; Scuseria, G. E.; Robb, M. A.; Cheeseman, J. R.; Scalmani, G.; Barone, V.; Mennucci, B.; Petersson, G. A.; Nakatsuji, H.; Caricato, M.; Li, X.; Hratchian, H. P.; Izmaylov, A. F.; Bloino, J.; Zheng, G.; Sonnenberg, J. L.; Hada, M.; Ehara, M.; Toyota, K.; Fukuda, R.; Hasegawa, J.; Ishida, M.; Nakajima, T.; Honda, Y.; Kitao, O.; Nakai, H.; Vreven, T.; Montgomery, J. A., Jr.; Peralta, J. E.; Ogliaro, F.; Bearpark, M.; Heyd, J. J.; Brothers, E.; Kudin, K. N.; Staroverov, V. N.; Kobayashi, R.; Normand, J.; Raghavachari, K.; Rendell, A.; Burant, J. C.; Iyengar, S. S.; Tomasi, J.; Cossi, M.; Rega, N.; Millam, J. M.; Klene, M.; Knox, J. E.; Cross, J. B.; Bakken, V.; Adamo, C.; Jaramillo, J.; Gomperts, R.; Stratmann, R. E.; Yazyev, O.;

Austin, A. J.; Cammi, R.; Pomelli, C.; Ochterski, J. W.; Martin, R. L.; Morokuma, K.; Zakrzewski, V. G.; Voth, G. A.; Salvador, P.; Dannenberg, J. J.; Dapprich, S.; Daniels, A. D.; Farkas; Foresman, J. B.; Ortiz, J. V.; Cioslowski, J.; Fox, D. J. Gaussian, Inc., Wallingford, CT, 2009.
(59) Agarwal, N.; Mishra, S. P.; Kumar, A.; Hung, C.-H.; Ravikanth, M. *Chem. Commun.* **2002**, 2642.
(60) Gupta, I.; Hung, C.-H.; Ravikanth, M. *Eur. J. Org. Chem.* **2003**, 4392.
(61) You, Y.; Daniels, T. S.; Dominiak, P. M.; Detty, M. R. *J. Porphyrins Phthalocyanines* **2007**, *11*.
(62) Zhu, Y.; Zhu, Y.-Z.; Song, H.-B.; Zheng, J.-Y.; Liu, Z.-B.; Tian, J.-G. *Tetrahedron Lett.* **2007**, *48*, 5687.
(63) Macrae, C. F.; Bruno, I. J.; Chisholm, J. A.; Edgington, P. R.; McCabe, P.; Pidcock, E.; Rodriguez-Monge, L.; Taylor, R.; Streek, J. v. d.; Wood, P. A. *J. Appl. Crystallogr.* **2008**, *41*, 466−470.
(64) Improta, R.; Ferrante, C.; Bozio, R.; Barone, V. *Phys. Chem. Chem. Phys.* **2009**, *11*, 4664−4673.
(65) Govind, N.; Valiev, M.; Jensen, L.; Kowalski, K. *J. Phys. Chem. A* **2009**, *113*, 6041−6043.